DETECTION AND ISOLATION OF LEAKAGE AND VALVE FAULTS IN HYDRAULIC SYSTEMS IN VARYING LOADING CONDITIONS, PART 1: GLOBAL SENSITIVITY ANALYSIS

Jarmo Nurmi and Jouni Mattila

Tampere University of Technology, Department of Intelligent Hydraulics and Automation, P.O. Box 589, 33101 Tampere, Finland

E-mail: jarmo.nurmi@tut.fi

Abstract

Model-based condition monitoring methods are widely used in condition monitoring. They usually rely on ad hoc approaches to verify the system model and then best practices are reported to detect the given set of faults. This first part of a two-piece paper introduces a generic Global Sensitivity Analysis-based approach that can be applied systematically to verify the model parameter sensitivities used for the model-based fault detection. The case study is a generic servo valve-controlled hydraulic cylinder with unknown loading condition which is then systematically analyzed with Global Sensitivity Analysis. The method shows valuable insight into systematic model verification and resulting fault detection in terms of showing the dominant sensitivity of the nominal flow rate and nominal pressure difference, and the exact sensitivities of 0-1 dm^3/min external and internal leakages on cylinder chamber pressures and velocity. In the second paper, an Unscented Kalman Filter-based Fault Detection and Isolation scheme for leakage and valve faults of a generic servo valve-controlled hydraulic cylinder is devised and fault patterns are presented.

Keywords: global sensitivity analysis, fault detection, model verification, Sobol' indices

1 Introduction

In a fault detection process, system condition is constantly observed and decisions are made whether the system has faults. Once a fault is detected, a fault isolation process takes over and localizes the cause of the fault.

To avoid false alarms (or false positives), in model-based condition monitoring it is important to verify the model to be as accurate as possible. A Global Sensitivity Analysis (GSA, Saltelli et al. 2008) helps in the verification, since it reveals the most sensitive parameters of the system in a systematic way. By focusing efforts on improving the sensitive parameters, a more robust model is reached. The GSA can also reveal the sensitivity of faults on system outputs, which is useful for fault detection purposes.

Model sensitivity can be analyzed locally. For instance, a Local Sensitivity Analysis (LSA) to a nonlinear variable displacement axial piston pump model was applied to study parameter sensitivities and to reduce model order (Kim et al., 1987), and to a linear water quality model (Pastres et al., 1997). In LSA, parameters are deviated individually from their nominal values, which can be performed analytically with Eq. (1) if the model output is differentiable and otherwise numerically with Eq. (2):

$$S_i = \frac{\partial Y}{\partial X_i}, \qquad i = \{1,2,3,\dots,k\} \tag{1}$$

$$S_i = \frac{Y - f(X_1, X_2, X_3, \dots, X_i + \Delta X_i, \dots, X_k)}{\Delta X_i} \tag{2}$$

where S_i is the sensitivity of output $Y = f(X_1, X_2, X_3, \dots, X_k)$ to a change in parameter X_i.

Thus LSA sensitivities are valid in close proximity of nominal parameters. Therefore, GSA is more applicable to nonlinear models since GSA sensitivities are valid in a wider parameter space. Previously, GSA has been used in studying, for example the sensitive forces in a pipe bend and parameters in a dam-break experiment (Hall. et al., 2009), and the parameters in water hammer model (Kaliatka et al., 2009). The GSA method of this paper is the variance-based Sobol' indices because it is simpler to implement than for instance the Fourier Amplitude Sensitivity Test (FAST).

Current studies on model-based condition monitoring rely on an ad hoc approach to find the best ways to detect faults and to verify the model parameters. Our proposal in this paper is the systematic utilization of GSA to verify the system model and to find the best practices to detect faults.

This paper is organized as follows. In Section 2, the mechanism of a generic valve-controlled hydraulic cylinder that drives a manipulator joint is presented. Then the corresponding test bed is introduced and modelled. In Section 3, the GSA algorithm and its implementation with Monte Carlo methods are described. In Section 4, the GSA is applied to the test bed and the results are discussed.

2 Modelling and Test Bed

The objective of the fault detection and isolation scheme that is devised in part 2 on the basis of part 1 is that it is applicable to a generic valve-controlled cylinder that drives any of the n-DOF manipulator joints, see Fig. 1:.

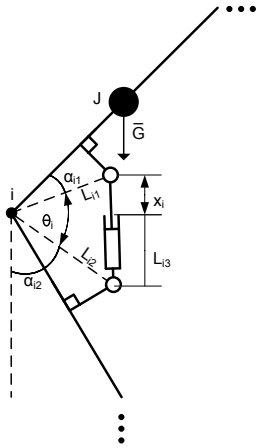

Fig. 1: *A manipulator joint driven by a hydraulic cylinder.*

The piston position of the ith cylinder is given by the law of cosines:

$$x_{\mathrm{i}}(\theta_{\mathrm{i}}) = \sqrt{L_{\mathrm{i1}}^2 + L_{\mathrm{i2}}^2 - 2L_{\mathrm{i1}}L_{\mathrm{i2}}\cos\theta_{\mathrm{i}}} - L_{i3} \tag{3}$$

Piston velocity of the ith cylinder can be differentiated from Eq. (3):

$$\dot{x}_{\mathrm{i}}(\theta_{\mathrm{i}}) = r_{\mathrm{i}}(\theta_{\mathrm{i}})\dot{\theta}_{\mathrm{i}} \tag{4}$$

where $\dot{\theta}_{\mathrm{i}}$ is the angular velocity of the joint and the torque arm of the ith cylinder is given by:

$$r_{\mathrm{i}}(\theta_{\mathrm{i}}) = \frac{L_{\mathrm{i1}}L_{\mathrm{i2}}\sin\theta_{\mathrm{i}}}{\sqrt{L_{\mathrm{i1}}^2 + L_{\mathrm{i2}}^2 - 2L_{\mathrm{i1}}L_{\mathrm{i2}}\cos\theta_{\mathrm{i}}}} \tag{5}$$

Consider an open chain manipulator system that consists of n cylinders. The piston velocities of all cylinders can be presented compactly with matrix notation:

$$\dot{\boldsymbol{x}} = \mathbf{R}(\boldsymbol{\theta})\dot{\boldsymbol{\theta}} = \begin{bmatrix} \mathrm{r}_1(\theta_1) & 0 & \cdots & 0 \\ 0 & \mathrm{r}_2(\theta_2) & \cdots & 0 \\ \vdots & \cdots & \ddots & \vdots \\ 0 & 0 & \cdots & \mathrm{r}_{\mathrm{n}}(\theta_{\mathrm{n}}) \end{bmatrix} \dot{\boldsymbol{\theta}} \tag{6}$$

The torques acting on the joints expressed with linear actuator coordinates are (Beiner and Mattila, 1999):

$$\begin{aligned} \boldsymbol{\tau}_{\mathrm{cyl}} &= \mathbf{R}(\boldsymbol{\theta})\boldsymbol{F} \\ &= \mathbf{J}(\boldsymbol{\theta})\mathbf{R}(\boldsymbol{\theta})^{-1}\ddot{\boldsymbol{x}} - \mathbf{J}(\boldsymbol{\theta})\mathbf{R}(\boldsymbol{\theta})^{-1}\dot{\mathbf{R}}(\boldsymbol{\theta})\mathbf{R}(\boldsymbol{\theta})^{-1}\dot{\boldsymbol{x}} + \boldsymbol{V}(\boldsymbol{\theta},\dot{\boldsymbol{\theta}}) \\ &+ \boldsymbol{G}(\boldsymbol{\theta}) \end{aligned} \tag{7}$$

where $\mathbf{R}(\boldsymbol{\theta})\boldsymbol{F}$ consists of cylinder actuator torques, $\boldsymbol{V}(\boldsymbol{\theta},\dot{\boldsymbol{\theta}})$ consists of torques caused by the Coriolis effect and centrifugal force, and $\boldsymbol{G}(\boldsymbol{\theta})$ is the vector of gravitational torques.

2.1 Case Study –Test Bed

The GSA is applied to a hydraulic boom called Single Axis Mock-up (SAM), shown in Fig. 2:.

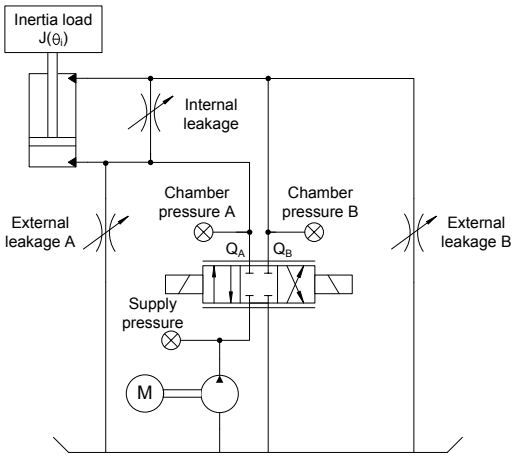

Fig. 2: *The hydraulic diagram of the SAM.*

The SAM has a 4/3-directional valve that controls the joint cylinder. Three restrictor valves are used to emulate external leakages ('External leakage A' and 'External leakage B') and internal leakage ('Internal leakage'). The external leakage emulates fluid leakage to the environment due to a broken hose, pipe or a failed coupling, while the internal leakage arrangement emulates cylinder seal failure. The system components are listed to Appendix 1, Table 9:. The SAM, with a 4.5 Hz maximum hydraulic natural frequency (Fig. 4:), is illustrated in Fig. 3:.

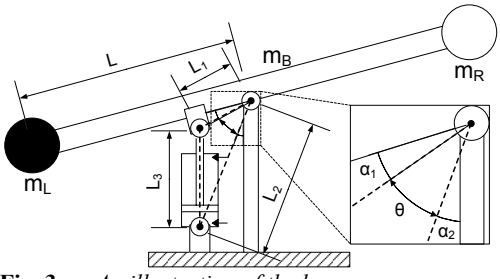

Fig. 3: *An illustration of the boom.*

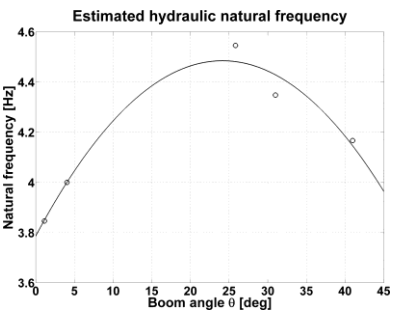

Fig. 4: *The estimated hydraulic natural frequency of SAM.*

2.2 Case Study –Test Bed Model

The mathematical model is divided into hydraulic system equations, motion equations of the boom, and then the entire model is presented in a continuous-time and in a discretized state space form.

2.2.1 Hydraulic System Equations

Equations (8) and (9) describing the change in chamber pressures are as follows (Watton, 1989):

$$\dot{p}_A = \frac{B_{effA}}{V_{0A} + A_A x}(Q_A(\mathrm{p_A}, \mathrm{x_s}) - A_A \dot{x}) \tag{8}$$

$$\dot{p}_B = \frac{B_{effB}}{V_{0B} + A_B(x_{max} - x)}(Q_B(\mathrm{p_B}, \mathrm{x_s}) + A_B \dot{x}) \tag{9}$$

where B_{effX} is the effective bulk modulus in chamber X (for X = A, B), $V_{0\mathrm{X}}$ is the volume in chamber X, A_{X} is the area in chamber X, Q_{X} is the flow sum to and from chamber X, x_{max} is the cylinder stroke, x is the piston position and $\dot{x}$ denotes velocity.

The algebraic equations for flows $Q_{\mathrm{A}}(\mathrm{p_A}, \mathrm{x_s})$ and $Q_{\mathrm{B}}(\mathrm{p_B}, \mathrm{x_s})$ with the flow into the cylinder being positive can be written as follows:

$$Q_A(\dots) = \begin{cases} K_{vPA}(x_s + offset)\sqrt{|p_S - p_A|}sgn(p_S - p_A) + Q_{leakA}, & x_s + offset > 0 \\ -K_{vAT}(-x_s + offset)\sqrt{|p_A - p_T|}sgn(p_A - p_T) + Q_{leakA}, & x_s + offset < 0 \\ 0, & x_s = -offset \end{cases} \tag{10}$$

$$Q_{\mathrm{B}}(\dots) = \begin{cases} -\mathrm{K_{vBT}}(\mathrm{x_s} + \mathrm{offset})\sqrt{|\mathrm{p_B} - \mathrm{p_T}|}\mathrm{sgn}(\mathrm{p_B} - \mathrm{p_T}) + Q_{leakB}, & x_s + \mathrm{offset} > 0 \\ \mathrm{K_{vPB}}(-\mathrm{x_s} + \mathrm{offset})\sqrt{|\mathrm{p_S} - \mathrm{p_B}|}\mathrm{sgn}(\mathrm{p_S} - \mathrm{p_B}) + Q_{leakB}, & x_s + \mathrm{offset} < 0 \\ 0, & x_s = -offset \end{cases} \tag{11}$$

where $\mathrm{K_{vX}}$ is flow coefficient in notch X, for X = PA, AT, BT and PB, x_{s} is the spool position, offset denotes the deviation of the valve spool from its correct position, p_{S} is the supply pressure, p_{A} is the pressure A, p_{T} is the tank pressure and p_{B} is the pressure B. The flow coefficients are defined as follows:

$$K_{\mathrm{vX}} = \frac{Q_{N,X}}{\sqrt{\Delta \mathrm{p_{N,X}}}} \tag{12}$$

where $Q_{\mathrm{N,X}}$ is the nominal flow rate and $\Delta \mathrm{p_{N,X}}$ is the nominal pressure difference in notch X.

The terms Q_{leakA} and Q_{leakB} are laminar leakage flows, present when the spool position is between -1 % and 1 % of its maximum:

$$\begin{cases} Q_{leakA} = K_{vPA,leak}(p_S - p_A) - K_{vAT,leak}(p_A - p_T), & |\mathrm{x_s}| < 0.01 \\ 0, & otherwise \end{cases} \tag{13}$$

$$\begin{cases} Q_{leakB} = K_{vPB,leak}(p_S - p_B) - K_{vBT,leak}(p_B - p_T) & |\mathrm{x_s}| < 0.01 \\ 0, & otherwise \end{cases} \tag{14}$$

where $K_{vX,leak}$ are the leakage flow coefficients.

The spool x_s dynamics are modelled with the 2nd order differential equation:

$$\ddot{x}_s = K\omega_n^2 u - 2\omega_n d_r \dot{x}_s - \omega_n^2 x_s \tag{15}$$

2.2.2 Motion Equations of the Boom

The piston position $x(\theta)$ is calculated according to Eq. (3) and the velocity $\dot{x}(\theta)$ according to Eq. (4).

We calculate the angular acceleration of the boom $\ddot{\theta}$ by dividing the sum of torques acting on the boom with total moment of inertia as follows:

$$\ddot{\theta} = \frac{\sum \overline{\tau}}{J_{\mathrm{tot}}} = \frac{\tau_{\mathrm{cyl}} + \tau_{\mathrm{mR}} - \tau_{\mathrm{mL}} - \tau_{\mathrm{B}}}{\frac{1}{12} m_{\mathrm{B}} {L_{\mathrm{B}}}^2 + m_{\mathrm{L}} L^2 + m_{\mathrm{R}} L^2} \tag{16}$$

where τ_{cyl} is the torque generated by the cylinder, τ_{mR} and τ_{mL} are the torques caused by the load masses on the right and left, respectively, and τ_{B} is the torque produced by the boom, since the boom is not jointed to the base from its center of gravity. The total moment of inertia J_{tot} consists of the load masses m_{L} and m_{R} at a distance L from the center of rotation, and of the boom's moment of inertia with mass m_{B} and length L_{B}.

The friction force F_{μ} is as follows (Canudas de Wit et al., 1995):

$$F_{\mu}(\dot{x}, \mathrm{z}) = \sigma_0 z + \sigma_1 \underbrace{[\frac{\sigma_0 |\dot{x}|}{[\mathrm{F_C} + (\mathrm{F_S} - \mathrm{F_C})\mathrm{e}^{-(\dot{x}/\mathrm{v_s})^2}} \mathrm{z}]}_{\dot{z}} + b\dot{x} \tag{17}$$

where z is the bending of the cylinder seal, σ_0 is the stiffness of the seal, σ_1 is the damping coefficient and b is the viscous friction coefficient. This friction model includes the stick-slip phenomenon. For more information on the dynamics of state variable z refer to the original publication (Canudas de Wit et al., 1995). The relation between pressure levels and friction force was neglected.

2.2.3 State Space Representation of the Model

The entire model can be presented compactly in state space form. The states of the system are:

$$\boldsymbol{x} = [p_{\mathrm{A}}, p_{\mathrm{B}}, x_{\mathrm{s}}, \dot{x}_{\mathrm{s}}, x, \dot{x}, z]^{\mathrm{T}} = [x_1, x_2, x_3, x_4, x_5, x_6, x_7]^{\mathrm{T}} \tag{18}$$

The continuous-time state space representation is then:

$$\begin{bmatrix} \dot{x}_1 \\ \dot{x}_2 \\ \dot{x}_3 \\ \dot{x}_4 \\ \dot{x}_5 \\ \dot{x}_6 \\ \dot{x}_7 \end{bmatrix} = \begin{bmatrix} \frac{B_{\mathrm{effA}}}{V_{0\mathrm{A}} + A_{\mathrm{A}} x_5}(Q_{\mathrm{A}}(\mathrm{x_1}, \mathrm{x_3}) - A_{\mathrm{A}} x_6) \\ \frac{B_{\mathrm{effB}}}{V_{0\mathrm{B}} + A_{\mathrm{B}}(x_{\mathrm{max}} - x_5)}(Q_{\mathrm{B}}(\mathrm{x_2}, \mathrm{x_3}) + A_{\mathrm{B}} x_6) \\ x_4 \\ K\omega_{\mathrm{n}} u - 2\omega_{\mathrm{n}} d_{\mathrm{r}} x_4 - \omega_{\mathrm{n}}^2 x_3 \\ x_6 \\ m_{\mathrm{reduced}}^{-1}(x_1 A_{\mathrm{A}} - x_2 A_{\mathrm{B}} - F_{\mu}(\mathrm{x_6}, \mathrm{x_7}) - F_{\mathrm{ext}}) \\ x_6 - \sigma_0 |x_6| [F_{\mathrm{c}} + (F_{\mathrm{S}} - F_{\mathrm{c}}) e^{-(x_6/v_{\mathrm{s}})^2}]^{-1} x_7 \end{bmatrix} \tag{19}$$

where m_{reduced} is the reduced mass on the cylinder and F_{ext} is the external force which can be written as:

$$m_{\mathrm{reduced}}(\theta) = \frac{J_{\mathrm{tot}}}{r^2(\theta)} \tag{20}$$

$$F_{\mathrm{ext}} = \frac{-\tau_{\mathrm{mR}} + \tau_{\mathrm{mL}} + \tau_{\mathrm{B}}}{r} \tag{21}$$

The continuous-time state space representation can be transformed to discrete-time with sampling time T with Euler's forward method:

$$\begin{bmatrix} x_1(k+1) \\ x_2(k+1) \\ x_3(k+1) \\ x_4(k+1) \\ x_5(k+1) \\ x_6(k+1) \\ x_7(k+1) \end{bmatrix} = \begin{bmatrix} x_1(k) \\ x_2(k) \\ x_3(k) \\ x_4(k) \\ x_5(k) \\ x_6(k) \\ x_7(k) \end{bmatrix} +$$

$$T \begin{bmatrix} \frac{B_{\mathrm{effA}}}{A_{\mathrm{A}} x_5(k) + V_{0\mathrm{A}}} (Q_{\mathrm{A}}(\mathrm{x}_1(k), \mathrm{x}_3(k)) - A_{\mathrm{A}} x_6(k)) \\ \frac{B_{\mathrm{effB}}}{A_{\mathrm{A}}(x_{\max} - x_5(k)) + V_{0\mathrm{B}}} (Q_{\mathrm{B}}(\mathrm{x}_2(k), \mathrm{x}_3(k)) + A_{\mathrm{B}} x_6(k)) \\ x_4(k) \\ K\omega_{\mathrm{n}} u(k) - 2\omega_{\mathrm{n}} d_r x_4(k) - \omega_{\mathrm{n}}^2 x_3(k) \\ x_6(k) \\ m_{\mathrm{reduced}}^{-1}(x_1(k) A_{\mathrm{A}} - x_2(k) A_{\mathrm{B}} - F_{\mu}(\mathrm{x}_6(k), \mathrm{x}_7(k)) - F_{\mathrm{ext}}) \\ x_6(k) - \sigma_0 |x_6(k)| \left[F_{\mathrm{c}} + (F_{\mathrm{S}} - F_{\mathrm{c}}) e^{-\left(\frac{x_6(k)}{v_{\mathrm{s}}}\right)^2} \right]^{-1} x_7(k) \end{bmatrix} \tag{22}$$

3 Global Sensitivity Analysis

A Global Sensitivity Analysis (GSA) method called Sobol' indices, its computation procedure and its usefulness for condition monitoring and model verification are introduced in this section.

3.1 Sobol' Indices Method

The premises for the variance-based Sobol' indices method are as follows (Saltelli et al., 2008, pp. 160-163). Consider the model to be a square-integrable function $\boldsymbol{Y} = \mathrm{f}(\boldsymbol{X})$ which can be divided into summands of increasing dimensionality:

$$\begin{aligned} &\mathrm{f}(X_1, X_2, X_3, \dots X_{\mathrm{k}}) \\ &= \mathrm{f}_0 + \sum_{\mathrm{i}=1}^{\mathrm{k}} \mathrm{f}_{\mathrm{i}}(X_{\mathrm{i}}) \\ &+ \sum_{\mathrm{i}=1}^{\mathrm{k}} \sum_{\mathrm{j}=\mathrm{i}+1}^{\mathrm{k}} \mathrm{f}_{\mathrm{ij}}(X_{\mathrm{i}}, X_{\mathrm{j}}) + \cdots \\ &+ \mathrm{f}_{1\dots\mathrm{k}}(X_1, X_2, X_3, \dots X_{\mathrm{k}}) \end{aligned} \tag{23}$$

where k is the number of parameters and X_{k} is the random parameter k.

Equation (23) has a total of 2^{k} terms and infinite solutions. Sobol' proposed one solution, which decomposes the function $\mathrm{f}(\boldsymbol{X})$ into conditional expectations. The first three terms can be written as:

$$\mathrm{f}_0 = \mathrm{E}(\boldsymbol{Y}) \tag{24}$$

$$\mathrm{f}_{\mathrm{i}} = \mathrm{E}(\boldsymbol{Y}|X_{\mathrm{i}}) - \mathrm{E}(\boldsymbol{Y}) \tag{25}$$

$$\mathrm{f}_{\mathrm{ij}} = \mathrm{E}(\boldsymbol{Y}|X_{\mathrm{i}}, X_{\mathrm{j}}) - \mathrm{f}_{\mathrm{i}} - \mathrm{f}_{\mathrm{j}} - \mathrm{E}(\boldsymbol{Y}) \tag{26}$$

where $\mathrm{E}(\boldsymbol{Y})$ denotes the expectation of model output $\boldsymbol{Y}$, $\mathrm{E}(\boldsymbol{Y}|X_{\mathrm{i}})$ is the conditional expectation of output $\boldsymbol{Y}$ given that input X_{i} is fixed to a certain value.

The variances of Eq. (24)-(26) have the following properties:

$$\mathrm{V}_0 = \mathrm{V}(\mathrm{f}_0) = 0 \tag{27}$$

$$\mathrm{V}_{\mathrm{i}} = \mathrm{V}(\mathrm{f}_{\mathrm{i}}) = \mathrm{V}[\mathrm{E}(\boldsymbol{Y}|X_{\mathrm{i}})] \tag{28}$$

$$\begin{aligned} &\mathrm{V}_{\mathrm{ij}} = \mathrm{V}(\mathrm{f}_{\mathrm{ij}}) \\ &= \mathrm{V}\left[\mathrm{E}\left(\boldsymbol{Y}\middle|X_{\mathrm{i}}, X_{\mathrm{j}}\right)\right] - \mathrm{V}[\mathrm{E}(\boldsymbol{Y}|X_{\mathrm{i}})] - \mathrm{V}[\mathrm{E}(\boldsymbol{Y}|X_{\mathrm{j}})] \end{aligned} \tag{29}$$

The conditional variance in Eq. (28) is used to calculate first order sensitivity indices, which is a measure on the main effect of parameter X_{i} on output $\boldsymbol{Y}$:

$$\mathrm{S}_{\mathrm{i}} = \frac{\mathrm{V}[\mathrm{E}(\boldsymbol{Y}|X_{\mathrm{i}})]}{\mathrm{V}(\boldsymbol{Y})} \tag{30}$$

where $\mathrm{V}(\boldsymbol{Y})$ is the unconditional variance of output $\boldsymbol{Y}$.

The interpretation for the term $\mathrm{V}[\mathrm{E}(\boldsymbol{Y}|X_{\mathrm{i}})]$ is that first the conditional expectation $\mathrm{E}(\boldsymbol{Y}|X_{\mathrm{i}})$ is calculated by fixing the input X_{i} to a certain value X_{i}^* and allowing other inputs to vary. Thus a complete representation for the conditional expectation is $\mathrm{E}_{\sim \mathrm{X}_{\mathrm{i}}}(\boldsymbol{Y}|X_{\mathrm{i}} = X_{\mathrm{i}}^*)$. The $\sim X_{\mathrm{i}}$ operator means that the expectation is calculated over every input excluding X_{i}. For k inputs that is a set $\{X_1, X_2, \dots, X_{\mathrm{i}-1}, X_{\mathrm{i}+1}, \dots, X_{\mathrm{k}}\}$. Then the variance of the expectation is calculated over different values of X_{i}. Thus the complete representation for the nominator is $\mathrm{V}_{\mathrm{X}_{\mathrm{i}}}[\mathrm{E}_{\sim \mathrm{X}_{\mathrm{i}}}(Y|X_{\mathrm{i}} = X_{\mathrm{i}}^*)]$.

The total order effects, which include the first order effect but also the terms that come from interaction between parameters, is derived from the law of total variance:

$$\mathrm{V}(\boldsymbol{Y}) = \mathrm{V}[\mathrm{E}(\boldsymbol{Y}|X_{\sim \mathrm{i}})] + \mathrm{E}[\mathrm{V}(\boldsymbol{Y}|X_{\sim \mathrm{i}})] \tag{31}$$

where the first term is the main effect and the remaining term the residual.

Then the total order sensitivity indices can be calculated with:

$$\mathrm{S}_{\mathrm{T}_{\mathrm{i}}} = \frac{\mathrm{E}[\mathrm{V}(\boldsymbol{Y}|X_{\sim \mathrm{i}})]}{\mathrm{V}(\boldsymbol{Y})} = 1 - \frac{\mathrm{V}[E(\boldsymbol{Y}|X_{\sim \mathrm{i}})]}{\mathrm{V}(\boldsymbol{Y})} \tag{32}$$

where the latter equality is obtained from Eq. (31) by solving it for $\mathrm{E}[\mathrm{V}(\boldsymbol{Y}|X_{\sim \mathrm{i}})]$ and placing it to the former equality.

In Eq. (32), $\mathrm{E}[\mathrm{V}(\boldsymbol{Y}|X_{\sim \mathrm{i}})]$ is a term that contains the variance of $\boldsymbol{Y}$ that would be left if all inputs but X_{i} could be fixed (X_{i} would be allowed to vary). Thus, diving $\mathrm{E}[\mathrm{V}(\boldsymbol{Y}|X_{\sim \mathrm{i}})]$ by $\mathrm{V}(\boldsymbol{Y})$ gives the proportion of the variance that is caused by X_{i}. The term $\mathrm{V}[\mathrm{E}(\boldsymbol{Y}|X_{\sim \mathrm{i}})]$ contains the variance that would disappear from $\mathrm{V}(\boldsymbol{Y})$ if all inputs but X_{i} could be fixed.

3.2 Computing Sobol' Indices

The analytical computation of Sobol' indices of differential equation models is not possible. From Saltelli (2002) and Saltelli et al. (2008, pp. 164-167) a procedure for computing sensitivity indices is reached.

Consider two matrices $\mathbf{X}_1$ and $\mathbf{X}_2$ which are of size N x k. N is the sample size (the number of simulations), and k is the amount of parameters that are randomly varied. In $\mathbf{X}_1$ and $\mathbf{X}_2$ each row m, for example $\boldsymbol{X}_1^{\mathrm{m}}$ with $\mathrm{m} = \{1,2,3,\dots,\mathrm{N}\}$, corresponds to one simulation with k random inputs in the columns. The inputs are varied using quasi-random numbers from the Sobol' sequence (Sobol' & Kucherenko, 2005), which produces more accurate sensitivity indices than pseudorandom numbers drawn randomly.

Simulating with input matrices $\mathbf{X}_1$ and $\mathbf{X}_2$ N times, two output matrices $\mathbf{Y}_1 = \mathrm{f}(\mathbf{X}_1)$ and $\mathbf{Y}_2 = \mathrm{f}(\mathbf{X}_2)$ of size N x M are created, where M is the number of outputs. For $\boldsymbol{Y}_1$ and $\boldsymbol{Y}_2$ the estimated variances are:

$$\widehat{\mathrm{V}}(\mathbf{Y}_1) = \frac{1}{N}\sum_{\mathrm{m}=1}^{\mathrm{N}} \mathrm{f}^2(\boldsymbol{X}_1^{\mathrm{m}}) - \hat{\mathrm{f}}_1^2 \tag{33}$$

$$\widehat{\mathrm{V}}(\mathbf{Y}_2) = \frac{1}{N}\sum_{\mathrm{m}=1}^{\mathrm{N}} \mathrm{f}^2(\boldsymbol{X}_2^{\mathrm{m}}) - \hat{\mathrm{f}}_2^2 \tag{34}$$

where the squared expectation estimates are:

$$\hat{\mathrm{f}}_1^2 = \frac{1}{N}\sum_{\mathrm{m}=1}^{\mathrm{N}} \mathrm{f}(\boldsymbol{X}_1^{\mathrm{m}}) f(\boldsymbol{X}_2^{\mathrm{m}}) \tag{35}$$

$$\hat{\mathrm{f}}_2^2 = (\frac{1}{N}\sum_{\mathrm{m}=1}^{\mathrm{N}} \mathrm{f}(\boldsymbol{X}_2^{\mathrm{m}}))^2 \tag{36}$$

Equation (33) and Eq. (34) are used for computing first and total order indices, respectively.

We introduce input matrix $\mathbf{X}_{3\mathrm{i}}$ for calculating the nominators in Eq. (30) and (32). Matrix $\mathbf{X}_{3\mathrm{i}}$ has the same values as $\mathbf{X}_2$ except that the i^{th} column is taken from matrix $\mathbf{X}_1$. The first order sensitivity indices are:

$$\mathrm{S}_{\mathrm{i}} = \frac{\mathrm{V}[\mathrm{E}(\boldsymbol{Y}|X_{\mathrm{i}})]}{\mathrm{V}(\boldsymbol{Y})} = \frac{\frac{1}{N}\sum_{\mathrm{m}=1}^{\mathrm{N}} \mathrm{f}(\boldsymbol{X}_1^{\mathrm{m}})\,\mathrm{f}(\boldsymbol{X}_{3\mathrm{i}}^{\mathrm{m}}) - \hat{\mathrm{f}}_1^2}{\frac{1}{N}\sum_{\mathrm{m}=1}^{\mathrm{N}} \mathrm{f}^2(\boldsymbol{X}_1^{\mathrm{m}}) - \hat{\mathrm{f}}_1^2} \tag{37}$$

In the scalar product $\mathrm{f}(\boldsymbol{X}_1^{\mathrm{m}})\mathrm{f}(\boldsymbol{X}_{3\mathrm{i}}^{\mathrm{m}})$ the columns for X_{i} are the same. If X_{i} is influential, high and low values of outputs $\mathrm{f}(\boldsymbol{X}_1^{\mathrm{m}})$ and $\mathrm{f}(\boldsymbol{X}_{3\mathrm{i}}^{\mathrm{m}})$ are associated (a high value multiplied by a high value or a low value multiplied by a low value) and thus produce a higher value for the variance when the terms in the scalar product are added together. If X_i is a non-influential input, the high and low values of $\mathrm{f}(\boldsymbol{X}_1^{\mathrm{m}})$ and $\mathrm{f}(\boldsymbol{X}_{3\mathrm{i}}^{\mathrm{m}})$ are randomly associated, thus resulting in a lower value for the nominator.

The total order sensitivity indices are:

$$\begin{aligned}\mathrm{S}_{\mathrm{T}_{\mathrm{i}}} &= 1 - \frac{\mathrm{V}[\mathrm{E}(\boldsymbol{Y}|X_{\sim \mathrm{i}})]}{\mathrm{V}(\boldsymbol{Y})} \\ &= 1 - \frac{\frac{1}{N}\sum_{\mathrm{m}=1}^{\mathrm{N}} \mathrm{f}(\boldsymbol{X}_2^{\mathrm{m}})\,\mathrm{f}(\boldsymbol{X}_{3\mathrm{i}}^{\mathrm{m}}) - \hat{\mathrm{f}}_2^2}{\frac{1}{N}\sum_{\mathrm{m}=1}^{\mathrm{N}} \mathrm{f}^2(\boldsymbol{X}_2^{\mathrm{m}}) - \hat{\mathrm{f}}_2^2}\end{aligned} \tag{38}$$

The explanation for Eq. (38) is that as values for $X_{\sim \mathrm{i}}$ are the same and only the input X_{i} is randomly varied, if X_{i} is influential, the values in the product $\mathrm{f}(\boldsymbol{X}_2^{\mathrm{m}})\mathrm{f}(\boldsymbol{X}_{3\mathrm{i}}^{\mathrm{m}})$ will be randomly associated and produce a lower value in the latter term. But taking into consideration that this low value is subtracted from one, a high value will be the result, thus indicating that this input is meaningful, and vice versa.

At the expense of increased computational costs increasing sample size N results in better sensitivity index estimates, the described method requires N(2+k) model runs.

3.3 Interpreting Sensitivity Indices from a Condition Monitoring Perspective

Sensitivity indices are used to rank parameters according to their sensitivities for model verification purposes (Saltelli et al. 2008, pp. 166-167):

- Inputs with the lowest total order sensitivity indices (near zero) causing the least variance to the output can be fixed at a value between their examined bounds without compromising the accuracy of the model.
- Inputs with the highest first order sensitivity indices should be a priority in model verification, because their correct values will reduce the variance in output Y the most.

Model parameter interactions can be studied too. The interactions mean that the effect of parameter changes on the output is different if the parameters are changed together as opposed to individually changing them and summing their effects. The differences $S_{\mathrm{T}_{\mathrm{i}}} -$

S_i and $1 - \sum_{i=1}^{k} S_i$ are direct measures of the interactions. They are zero for perfectly additive models but nonzero for non-additive models.

GSA results are useful for fault detection purposes. The sensitivity indices of fault parameters indicate if the fault can be detected, and at which output.

4 Global Sensitivity Analysis of the Single Axis Mock-up

The sensitivity of the system for parameter changes and leakage faults is studied in this section, both in transients and in steady state. The main objective was to extract information from the sensitivities for fault detection purposes.

The valve control signal was a step signal to 25 % opening. Only the extending movement of the cylinder was examined because we wanted to limit the range of the study. Moreover, the asymmetry of the cylinder might affect the results in retraction. The sample size N in both analyses was 10000, with a fixed 1-millisecond simulation step size. The examined outputs were pressures A, B and velocity.

4.1 Sensitivity for Parameter Changes

The sensitivity of the SAM for seven varying parameters (k = 7) and their respective ranges are examined (Table 1:) using the model in Eq. (19).

Table 1: Single Axis Mock-up parameters deviated in the GSA.

Parameter	Explanation	Lower bound	Upper bound
offset	Spool deviation from actual position	-5 %	5 %
$Q_{N,PA}$	Nominal flow rate in notch PA	15 L/min	35 L/min
$\Delta p_{N,PA}$	Nominal pressure difference in notch PA	5 bar	40 bar
$Q_{N,BT}$	Nominal flow rate in notch BT	15 L/min	35 L/min
$\Delta p_{N,BT}$	Nominal pressure difference in notch BT	5 bar	40 bar
B_{eff}	Effective bulk modulus	300 MPa	1200 MPa
b	Viscous friction coefficient	2000 Ns/m	5000 Ns/m

The parameters are assumed to be uniformly distributed. The lower and upper bounds are chosen so that they are reasonable. For instance, the nominal flow rate of the valve is 24 L/min, thus a 15-35 L/min range is suitable. The nominal pressure differences are chosen so that most valve types fall within the range. Valve offset is a calibration error or a deviation caused by a valve fault. The constant parameters that were identified, measured or taken from manufacturer data are listed in Appendix 2.

The first order indices in steady state (Fig. 5:), including errors bounds calculated with a re-sampling method (bootstrapping), Archer et al. (1997), show how much variance in pressures and velocity is caused by individual parameters alone. The effective bulk modulus causes minor output variance. This is entirely intuitive because B_{eff} is a parameter that affects the natural frequency of the system and only has an effect on pressures or velocity in transients. This can be verified by setting either one of the pressure differential equations to zero to find the steady state pressures. Viscous friction coefficient b has insignificant magnitude, as indicated by the negligible sensitivity index b.

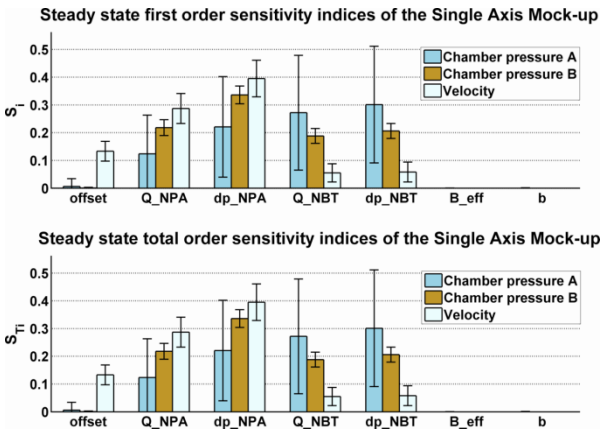

Fig. 5: *The first and total order sensitivity indices in steady state.*

Table 2: The ranking of parameters according to their first order indices.

Ranking	p_A	p_B	v
1	$\Delta p_{N,BT}$	$\Delta p_{N,PA}$	$\Delta p_{N,PA}$
2	$Q_{N,BT}$	$Q_{N,PA}$	$Q_{N,PA}$
3	$\Delta p_{N,PA}$	$\Delta p_{N,BT}$	*offset*
4	$Q_{N,PA}$	$Q_{N,BT}$	$\Delta p_{N,BT}$
5	*offset*	*offset*	$Q_{N,BT}$
6	B_{eff}	B_{eff}	B_{eff}
7	b	b	b

Table 2: ranks the parameters from Fig. 5:. It shows that the pressure variance is mostly captured by nominal pressure differences and flow rates. Notch BT parameters cause the most variance to pressure p_A, where as notch PA parameters are responsible for most of the variance to pressure p_B. The reason becomes clear from the steady state pressures:

$$p_{ssA} = \frac{F_{ext}A_A A_B K_{vBT}^2 + A_B^3 K_{vPA}^2 p_S + A_A^2 A_B K_{vBT}^2 p_T}{A_A^3 K_{vBT}^2 + A_B^3 K_{vPA}^2} \quad (39)$$

$$p_{ssB} = \frac{-F_{ext}K_{vPA}^2 A_B^2 + A_A A_B^2 K_{vPA}^2 p_S + A_A^3 K_{vBT}^2 p_T}{A_A^3 K_{vBT}^2 + A_B^3 K_{vPA}^2} \quad (40)$$

The steady state Eq. (39) can be derived by setting the pressure differential Eq. in (8) and (9) to zero and solving both for velocity. Then equating the resulting equations, replacing p_B with p_A calculated from the steady state motion equation of the piston, in Eq. (19), and finally solving for p_A and assuming that the friction force is included in the external force F_{ext} gives Eq. (39). Equation (40) is obtained likewise.

A difference in the steady state pressure equations is that in Eq. (39) F_{ext} is multiplied by flow coefficient K_{vBT}^2 and by K_{vPA}^2 in Eq. (40). Therefore, it is clear that parameters in notch BT affect pressure A more than pressure B. Similarly, parameters in notch PA cause more variance to pressure B. The nominal pressure differences are more influential than nominal flow rate because nominal pressure differences are varied along a wider range.

The sensitivity indices show that valve offset is influential on steady state velocity, which is obvious since the offset affects valve opening. The ranks for rest of the parameters affecting velocity are fairly intuitive.

For a measure of interactions between parameters, we sum up the first order indices of each parameter for each output. The results are presented in Table 3:. The interactions among parameters are negligible for each output, which means that the total order indices (Fig. 5:) do not differ remarkably from the first order indices. The unexplained part is five to seven percent in each output, which could be caused by estimation errors in the calculations. Increasing sample size could possibly reduce this.

Table 3: Parameter interactions in steady state.

Output	**Interaction measure:** $1 - \sum_{i=1}^{k} S_i$
p_A	0.0763
p_B	0.0507
v	0.0713

For computation of sensitivity indices in transients, an area plot is illustrative and the amount of interactions between parameters is visible. A general rule of thumb for reading the area plot is that the bigger the area of the parameter, the larger its effect is. Figure 6 presents interpolated first and total order indices for pressure A computed at time instants 0.05, 0.10, 0.20, 0.30, 0.5, 0.75, 1.0, 2.0, 3.0 and 4.0 seconds.

The first order indices in Fig. 6: show a sensitivity drop at 0.10 seconds to about 0.30 seconds. Particularly, the indices of valve nominal parameters in notch PA and the nominal flow rate of notch BT drop significantly. The figure shows that these are more significant parameters, especially at the beginning of the motion. After about a second all indices reach their steady state level.

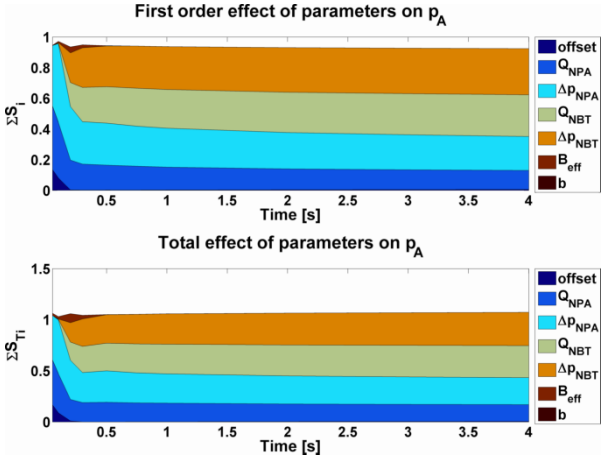

Fig. 6: *Area plot of pressure A first and total order sensitivity indices.*

The total order indices (Fig. 6:) drop similar to the first order indices. This indicates that the interactions between parameters are negligible. A difference between the first and total order indices is the influence of the somewhat larger effective bulk modulus.

Exact magnitudes are difficult to see from the area plot. Hence, the total order indices at selected time instants are gathered to Table 4:. We can see that effective bulk modulus B_{eff} has some impact on the system at time instants 0.20 and 0.30 seconds, even though its effect is smaller than the effects of nominal pressure differences and flow rates. This behaviour is expected because the system is in transient. What is interesting is that valve offset is very influential on pressure A few hundreds of a second into the experiment but loses its effect towards steady state. However, at no point is it more sensitive than the nominal parameters of notch PA.

Table 4: Pressure A total order sensitivity indices.

Time [s]	*offset*	$Q_{N,PA}$	$\Delta p_{N,PA}$	$Q_{N,BT}$	$\Delta p_{N,BT}$	B_{eff}	*b*
0.05	0.169	0.440	0.434	0.001	0.000	0.022	0.000
0.10	0.089	0.383	0.526	0.004	0.004	0.028	0.000
0.20	0.011	0.209	0.383	0.178	0.189	0.088	0.000
0.30	0.002	0.188	0.294	0.256	0.268	0.036	0.000
0.50	0.001	0.192	0.307	0.270	0.278	0.001	0.000
0.75	0.003	0.184	0.294	0.283	0.289	0.000	0.000
1.00	0.003	0.181	0.287	0.290	0.297	0.000	0.000
4.00	0.006	0.164	0.263	0.313	0.326	0.000	0.000

Other first and total order indices in transients are shown in Appendix 3. The pressure B first order indices behave opposite to pressure A indices. Specifically, the indices increase in the first few tenths of a second. The first order indices of velocity also behave differently; there is an increase in notch BT parameter indices and a decrease in notch PA parameter indices. The total order index of effective bulk modulus B_{eff} causes remarkable variance to pressure B, and the most variance to velocity at the beginning of the analysis. As time progresses, the effective bulk modulus loses its influence.

4.2 Sensitivity for Leakages

The analysis is carried out by studying the effects of internal leakage and external leakages in chambers A and B on pressures and velocity. The simultaneously varied parameters and their ranges are presented in Table 5:.

Table 5: Leakage sensitivity analysis parameters.

Parameter	Explanation	Lower bound [m^3/s $Pa^{-1/2}$]	Upper bound [m^3/s $Pa^{-1/2}$]
K_{int}	Internal leakage flow coefficient	0	$5.27*10^{-9}$
K_{extA}	External leakage A flow coefficient	0	$5.27*10^{-9}$
K_{extB}	External leakage B flow coefficient	0	$5.27*10^{-9}$

The upper bounds were chosen so that each leakage flow rate is 1 L/min with a pressure difference of 10 MPa, approximately 2.5 % of valve flow rate.

The leakage flows were modelled as turbulent and were added to the model at this stage. The flow equations (41)-(43) for internal leakage and external leakages A and B where the tank pressure is assumed to be zero are:

$$Q_{\text{int}} = K_{\text{int}}\sqrt{p_{\text{A}} - p_{\text{B}}} \tag{41}$$

$$Q_{\text{extA}} = K_{\text{extA}}\sqrt{p_{\text{A}}} \tag{42}$$

$$Q_{\text{extB}} = K_{\text{extB}}\sqrt{p_{\text{B}}} \tag{43}$$

Fig. 7: shows the first and total order effects of leakage faults on pressures and velocity in steady state. The first and total indices are approximately the same, the only difference being the effect of internal leakage on pressure A. This indicates only a minor amount of interactions between the leakage parameters K_{int}, K_{extA} and K_{extB}.

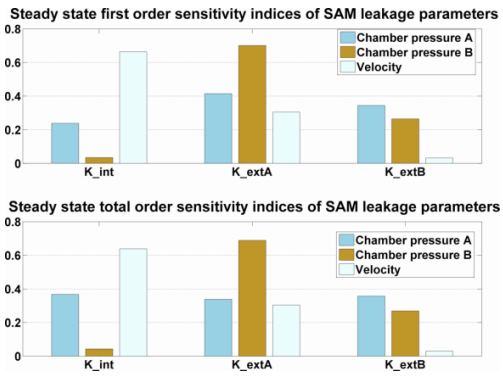

Fig. 7: *The first and total order effects of leakages in steady state.*

External leakage A causes remarkable variance to pressures A and B, and velocity. For explanation, consider the changes that occur as a consequence of external leakage A. When the leakage appears, it leads into a pressure drop in chamber A and a velocity decrease. As a consequence, the resistive pressure B drops. Pressure B is more sensitive to external leakage A than its own leakage because of the asymmetrical cylinder, the loading condition and the extending movement.

Consider the effects of external leakage B. That leakage reduces pressure B, which causes a mild increase in velocity (Fig. 7:). The influence on velocity is small, as external leakage B only lowers the motion-resistive pressure, and does not directly affect the driving pressure A. However, the results show that external leakage B, of course, (indirectly) affects pressure A through the motion equation. In this system, with its characteristics by the loading condition, the effect of external leakage B on pressure A was actually larger than on B.

Finally, look at the procedure when an internal leakage occurs. At first the internal leakage reduces pressure A and increases pressure B causing the velocity to decrease. However, the situation changes as time progresses since the increased flow into chamber B increases steady pressure B. Therefore, the pressure A also increases to balance. Finally, the velocity continues to drop, and internal leakage is clearly the most responsible for the variance in velocity (Fig. 7:). The influence of internal leakage on pressure B is minor, but could be larger in retraction. The leakage parameters are ranked to Table 6:.

Table 6: The ranking of leakage parameters according to their total order indices.

Ranking	p_{A}	p_{B}	v
1	K_{int}	K_{extA}	K_{int}
2	K_{extB}	K_{extB}	K_{extA}
3	K_{extA}	K_{int}	K_{extB}

The first order indices as a function of time for pressure A are presented in Fig. 8:. The external leakage A and internal leakage are the most influential leakages in the beginning, but as time progresses, and the flow-resistive pressure in chamber B develops, the external leakage B causes more and more variance to pressure A. At the same time the effect of external leakage A decreases and the effect of internal leakage increases.

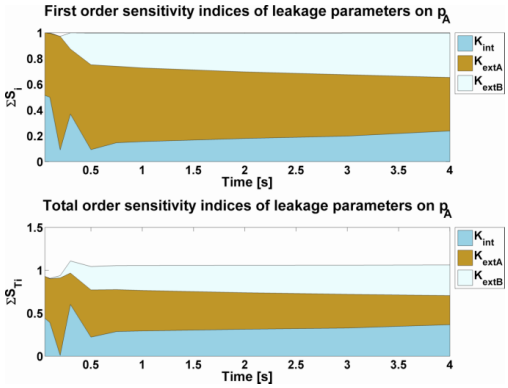

Fig. 8: *Pressure A first and total order sensitivity indices.*

The first order indices are shown with numerical figures in Table 7:.

Table 7: Pressure A first order sensitivity indices.

Time [s]	K_{int}	K_{extA}	K_{extB}
0.05	0.5141	0.4858	0.0000
0.10	0.4987	0.4994	0.0032
0.20	0.0908	0.8804	0.0000
0.30	0.3687	0.5042	0.1255
0.50	0.0928	0.6583	0.2454
0.75	0.1465	0.5928	0.2572
1.00	0.1552	0.5715	0.2695
4.00	0.2380	0.4145	0.3443

The total order indices are similar to the first order indices of K_{int} and K_{extB}, with the index of K_{extA} behaving differently. In the beginning, its influence increases as opposed to the decrease in first order indices, which flags interaction of external leakage A with other parameters. The total order indices are in Table 8:.

Table 8: Pressure A total order sensitivity indices.

Time [s]	K_{int}	K_{extA}	K_{extB}
0.05	0.4421	0.4872	0.000
0.10	0.3915	0.5107	0.0035
0.20	0.0098	0.9012	0.0264
0.30	0.6019	0.3660	0.1402
0.50	0.2219	0.5498	0.2718
0.75	0.2872	0.4882	0.2793
1.00	0.2944	0.4709	0.2906
4.00	0.3674	0.3385	0.3568

The first and total order sensitivity in transients for pressure B and velocity are in Appendix 4. In short, internal leakage causes the most variance to pressure B in the first tenth of a second; it is almost solely responsible for the variance. As time progresses, the influence of internal leakage decreases and the effects of external leakage A and B increase. The total order indices regarding pressure B and velocity are the same as the first order indices proving that there is no interaction between parameters. Throughout the analysis, the influence of external leakage B on velocity is nonexistent. As time progresses, internal leakage causes somewhat more variance to velocity, whereas external leakage A causes somewhat less.

5 Conclusions and Future Work

A generic Global Sensitivity Analysis-based approach that can be applied systematically to verify the model parameter sensitivities used for the model-based fault detection was presented in this paper. The GSA was applied to a valve-controlled asymmetrical hydraulic cylinder driving a 1-DOF manipulator joint to study its model parameter sensitivities. The studied parameters were the nominal flow rate and nominal pressure difference in the pressure and return notch of the valve, effective bulk modulus, valve spool offset and viscous friction coefficient. The sensitivity analysis was restricted to the extending motion.

Nominal flow rate and nominal pressure difference in the pressure notch of the valve were shown to be the most sensitive parameters to pressure or velocity responses regardless of whether the system was at steady state or transient. The second most sensitive parameters were the nominal flow rate and nominal pressure difference in the return notch. The effective bulk modulus was the third most sensitive parameter which was sensitive in transient pressure and velocity responses. The fourth most sensitive parameter was the valve offset which was sensitive in the steady state and transient velocity responses. The sensitivity of viscous friction was negligible throughout the analysis.

These results prove that flow coefficients should be identified to be as accurate as possible, since they had the largest sensitivity indices, and so the most effect on system outputs. Moreover, the identification of effective bulk modulus should be a second priority to facilitate model-based fault detection.

A leakage fault sensitivity analysis was also carried out to show the outputs from which the external leakage A, B and internal leakage could be best detected. The analysis proved that all leakage types can be detected with almost equal quality from the cylinder piston side pressure during transients or steady state during extension. From rod side pressure, all but the internal leakage in steady state and the external leakage B in transient are easily detectable. The rod side pressure was observed to be especially sensitive to internal leakage in transients. External leakage B was shown to be difficult to recognize from velocity in transients and steady state, so pressures are a prime candidate for detecting leakages.

The sensitivity indices can capture intuitively sensitive parameters and parameters whose sensitivity is more difficult to see. Whether the model is simple or complex, it is beneficial to systematically rank the parameters according to sensitivities since it decreases

the work needed in identifying parameters. The results of this part 1 will be used in part 2 where a scheme for detecting and isolating certain leakage and valve faults from a hydraulic system operating in various operating conditions is devised.

Acknowledgement

This work was funded by the Academy of Finland under the project 133273, Sensor network based intelligent condition monitoring of mobile machinery. The authors gratefully acknowledge the Academy of Finland for the financial support.

References

Archer, G., Saltelli, A. and **Sobol', I. M.** 1997. Sensitivity measures, ANOVA-like techniques and the use of bootstrap. Statistical computation and simulation, volume 58, issue 2, 1997, pp. 99-120.

Beiner, L. and **Mattila, J.** 1999. An improved pseudoinverse solution for redundant hydraulic manipulators. Robotica, volume 17, pp. 173-179.

Canudas de Wit, C., Olsson, H., Åström, K. J. and **Lischinsky, P.** 1995. A new model for control of systems with friction. IEEE transactions on automatic control, volume 40, issue 3, pp. 419-425.

Hall, J. W., Boyce, S. A., Wang, Y., Dawson, R. J., Tarantola, S. and **Saltelli, A.** 2009. Sensitivity Analysis for Hydraulic Models. Journal of hydraulic engineering, November 2009.

Kaliatka, A., Kopustinskas, V. and **Vaišnoras, M.** 2009. Water hammer model sensitivity study by the FAST method. Energetika, volume 55, issue 1, pp. 13-19.

Kim, S. D., Cho, H. S. and **Lee, C. O.** 1987. A parameter sensitivity analysis for the dynamic model of a variable displacement axial piston pump. Proc. of IMechE, volume 201, issue C4.

Pastres, R., Franco, D., Pecenik, G., Solidoro, C. and **Dejak, C.** 1997. Local sensitivity analysis of a distributed parameters water quality model. Reliability engineering & system safety, volume 57, issue 1, July 1997, pp. 21-30.

Saltelli, A. 2002. Making best use of model evaluations to compute sensitivity indices. Computer physics communications, volume 145, issue 2, 15 May 2002, pp. 280-297.

Saltelli, A., Ratto, M., Andres, T., Campolongo, F., Cariboni, J., Gatelli, D., Saisana, M. and **Tarantola, S.** 2008. Global sensitivity analysis: the primer. John Wiley & Sons. 292 p.

Sobol', I.M. and **Kucherenko, S.S.** 2005. On global sensitivity analysis of quasi-Monte Carlo algorithms. Monte Carlo methods and applications, volume 11, issue 1, pp. 1-9.

Sobol', I. M., Tarantola, S., Gatelli, D., Kucherenko, S.S. and **Mauntz, W.** 2007. Estimating the approximation error when fixing unessential factors in global sensitivity analysis. Reliability engineering & system safety, volume 92, issue 7, July 2007, pp. 957-960.

Watton, J. 1989. Fluid power systems: Modeling, simulation, analog and microcomputer control. Prentice Hall International (UK) Ltd. 490 p.

Appendix 1 - System Components

Table 9: The components in the SAM test bed.

Part	Model and specifications
Cylinder	Ø80/45-545
4/3-directional valve	Bosch Rexroth servo solenoid 4WRPEH 6 C3B24L-2X/G24K0/A1M (24 L/min @ 3.5 MPa)
Restrictor valve	Tognella needle valve FT257/2-38 (30 L/min @ 40 MPa)
Pressure transmitter	Trafag 8891.74 (0-25 MPa)
Pressure transmitter	Druck PTX 1400 (0-25 MPa)
Angle encoder	Heidenhain 376 886-0B (0.007 °/pulse)

Appendix 2 - Nomenclature and SAM Parameters

Parameter	Explanation	Value
A_A	Piston area	$\pi*(0.080)^2/4$ [m^2]
A_B	Piston rod area	$A_A - \pi*(0.045)^2/4$ [m^2]
b	Viscous friction	2500 Ns/m
d_r	Damping ratio	1
F_S	Static friction	4000 N
F_C	Coulomb's friction	1000 N
$\mathbf{J}(\theta)$	Moment of inertia matrix	-
K	Gain from control signal to spool position	0.1
$K_{vPA,leak}$	Leakage flow coeff. in notch PA	$1.9*10^{-12}$ $m^3/(sPa^{1/2})$
$K_{vBT,leak}$	Leakage flow coeff. in notch BT	$1.7*10^{-12}$ $m^3/(sPa^{1/2})$

$K_{vPB,leak}$, $K_{vAT,leak}$	Leakage flow coefficients in notches PB and AT	$1*10^{-12}$ $m^3/(sPa^{1/2})$
L	Load distance from the boom joint	1.9 m
L_B	Boom length	4.5 m
L_{i1}	Distance between upper cylinder joint and boom joint	0.30 m
L_{i2}	Distance between lower cylinder joint and boom joint	1.04 m
L_{i3}	Distance between lower and upper cylinder joints	0.84 m
m_B	Boom mass	297 kg
m_L	Left load mass	494 kg
m_R	Right load mass	0 kg
offset	Valve offset from center position	0
p_S	Supply pressure	10 MPa
$Q_{N,PA}$, $Q_{N,BT}$, $Q_{N,PB}$, $Q_{N,AT}$	Nominal flow rate in notch PA, BT, PB and AT	24 L/min
$\mathbf{R}(\theta)$	Torque arm matrix	-
r_B	Boom height	0.2 m
V_{0A}, V_{0B}	Volumes in A and B chambers	$2*10^{-4}$ m^3
v_s	Veloc. of min. frict.	0.01 m/s
x_{max}	Stroke	0.545 m
$\alpha_1 + \alpha_2$	See Fig. 3:	0.415 rad
$\Delta p_{N,PA}$, $\Delta p_{N,BT}$, $\Delta p_{N,PB}$, $\Delta p_{N,AT}$	Nominal pressure differences in notch PA, BT, PB and AT	3.5 MPa
θ	Joint angle	0.728 rad, cyl. retracted
σ_0	Friction coeff. 0	$4*10^6$ N/m
σ_1	Friction coeff. 1	$2*(\sigma_0*m_{redu})^{1/2}$
ω_n	Spool natural freq.	2*pi*20 rad/s

Appendix 3 - Sensitivity Indices of SAM

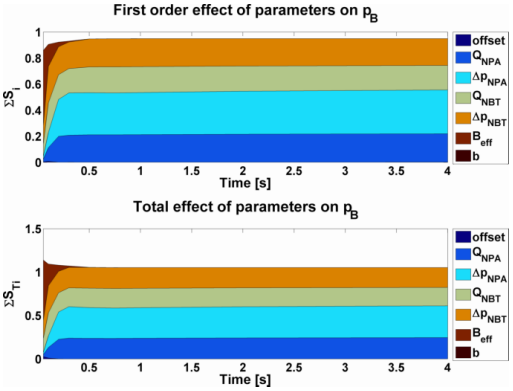

Fig. 9: *First and total order indices of parameters on pressure B.*

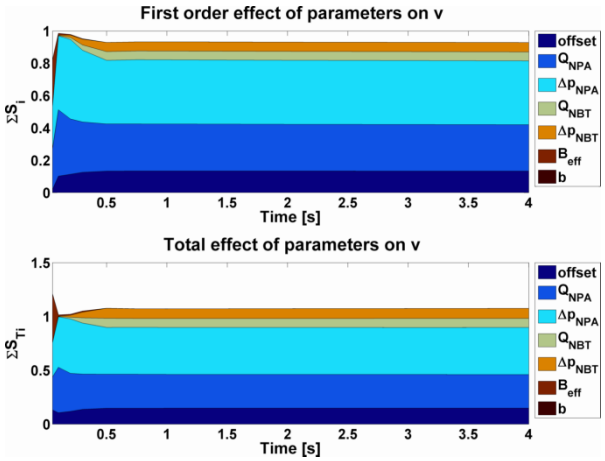

Fig. 10: *First and total order indices of parameters on velocity.*

Appendix 4 - Leakage Fault Sensitivity Indices of SAM

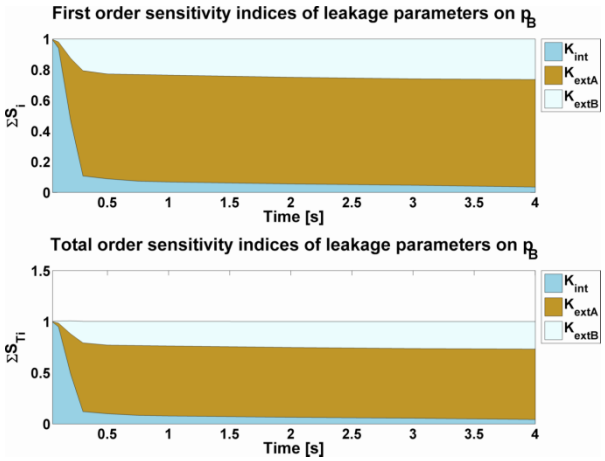

Fig. 11: *First and total order indices of leakage parameters on pressure B.*

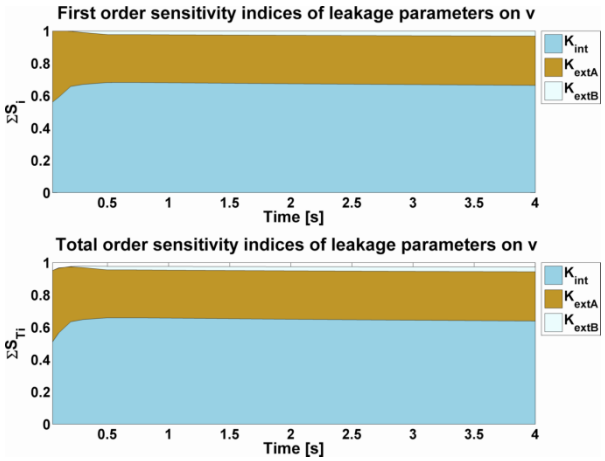

Fig. 12: *First and total order indices of leakage parameters on velocity.*